IOP Conf. Series: Materials Science and Engineering **408** (2018) 012027 doi:10.1088/1757-899X/408/1/012027

Dynamic Modelling of the Hovering Phase of a New V/STOL UAV and Verification of the PID Control Strategy

Xiaomeng Zhang* **and Weijun Wang**

Beihang University, Beijing, China

*15731168528@163.com

Abstract. This paper analyses the dynamics of a vertical/short take-off and landing (V/STOL) unmanned aerial vehicle (UAV), and obtains a nonlinear dynamics model. During the flight from vertical take-off to hovering, the roll moment, pitch moment and yaw moment are regarded as control inputs to linearize the nonlinear dynamic model to obtain the system transfer function. Finally, the control scheme of pitch angle during the flight from vertical take-off to hovering is developed, and the control scheme is verified by simulation. The simulation results reveal that the designed Proportional-Integration-Differential (PID) attitude controller can achieve stable control of the pitch attitude of the V/STOL drone during the hovering phase.

1. Introduction

Vertical/short take-off and landing (V/STOL) aircraft combines the advantages of fixed-wing aircraft and helicopter. In addition to achieving the speed of fixed-wing aircraft, V/STOL is also not subject to site constraints, which makes V/STOL aircraft of great significance in military and civil affairs.

V/STOL aircrafts are divided into two types by forms at the dynamic force: one is to achieve short-range vertical take-off and landing by deflecting thrust vector nozzles, such as "Harrier Jet"[1]; the other is through the tilting rotor, such as MV-22 "Osprey" [2]. However, aircrafts designed according to these two methods are complex in design and heavy. Therefore, these types are not suitable for unmanned aerial vehicle.

As shown in Figure 1. For the new V/STOL, the two pairs of propellers on the leading edge of the wing, combined with the help of the front propeller, produce the increasing effect of deflection slip flow of the propeller [3-4]. In this way, unconventional vertical take-off and hovering of the aircraft can be achieved. What's more, the increasing effect of deflection slip flow of the propeller can be also fully utilized by the design of the double slotted flap on the wing rudder surface. In general, the requirements of short-range take-off and landing drones, light and simple construction and low cost, are satisfied.

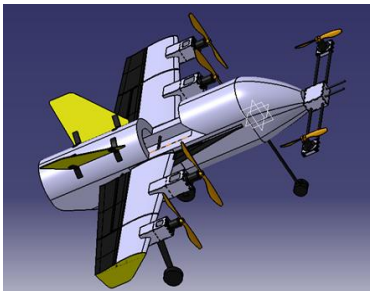

Figure 1. The schematic diagram of V/STOL aircraft

2. Analysis of dynamic equation

2.1. Coordinate system conversion

The earth coordinate system is attached to the surface of the earth, usually denoted by $OX_gY_gZ_g$, the usual earth coordinate system is the North-East-Earth coordinate system. That is, any point on the ground is regarded as the origin of the coordinate system, usually the position of the aircraft taking off. The body coordinate system is fixed to the aircraft. It is a dynamic coordinate system that changes continuously with position of the aircraft. The body coordinate system is generally represented by $OX_bY_bZ_b$.

According to the above setting, the transformation between the body coordinate system and the ground coordinate system is represented by the roll angle φ, the pitch angle θ, and the yaw angle ψ. By the vector transformation of Euler angles, the transformation from the body coordinate system to the earth coordinate system can be given by:

$$C_{\mathrm{b}}^{\mathrm{n}} = C_{\mathrm{z}}(\psi)C_{\mathrm{y}}(\theta)C_{\mathrm{x}}(\phi) \tag{1}$$

$$C_{\mathrm{b}}^{\mathrm{n}} = \begin{bmatrix} \cos(\theta)\cos(\psi) & -\cos(\phi)\sin(\psi)+\sin(\phi)\sin(\theta)\cos(\psi) & \sin(\phi)\sin(\psi)+\cos(\phi)\sin(\theta)\cos(\psi) \\ \cos(\theta)\sin(\psi) & \cos(\phi)\cos(\psi)+\sin(\phi)\sin(\theta)\sin(\psi) & -\sin(\phi)\cos(\psi)+\cos(\phi)\sin(\theta)\sin(\psi) \\ -\sin(\theta) & \sin(\phi)\cos(\theta) & \cos(\phi)\cos(\theta) \end{bmatrix} \tag{2}$$

Supposing: p, q, r are the angular velocities of the aircraft in the body coordinate system, and $\dot{\varphi}$, $\dot{\theta}$ $\dot{\psi}$ are the Euler angles velocities of the aircraft in the earth coordinate system. Based on the conversion relationship, it can be expressed that:

$$\begin{cases} \dot{\phi} = p + \left(r\cos(\phi) + q\sin(\phi)\right)\tan(\theta) \\ \dot{\theta} = q\cos(\phi) - r\sin(\phi) \\ \dot{\psi} = \dfrac{1}{\cos(\theta)}\left(r\cos(\phi) + q\sin(\phi)\right) \end{cases} \tag{3}$$

2.2. Linear dynamics equations

The movement of the aircraft in space is described by 6-DOF (Six Degrees Of Freedom) model. The linear velocity vector of the aircraft in the ground coordinate system is $V_E = [\dot{x}\ \dot{y}\ \dot{z}]^T$, the angular velocity vector in the body coordinate system is $W_b = [p\ q\ r]^T$. In the hovering state, only three forces, which are the force of the combination of propeller, wing and flap, the force of front propeller and gravity, need to be considered respectively. In the body coordinate system, the schematic diagram of force analysis in the hover state is depicted in figure 2.

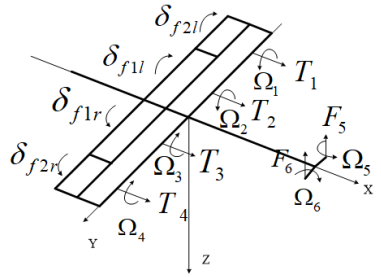

Figure 2. The schematic diagram of force analysis in the hovering state

The force of the combination of propeller, wing and flap acts on 1, 2, 3, and 4 points respectively, regarded as F_1, F_2, F_3, F_4. The propellers at the 2 and 3 positions turn inwards. The propellers at the 1 and 4 positions turn outward. The force of the forward propeller is applied at 5 and 6 points, turn outward too. The flap deflection angle is denoted by 'a 'and the aileron deflection angle is denoted by 'b '. It should be noted that in the process analysis of the present work, it is assumed that the flap and

the aileron deflection angles are fixed during the hovering process, that is to say, 'a' and 'b' are constant. Equations of force analysis in the body coordinate system are as follows:

$$\begin{cases} f_x = \cos(a)(F_2 + F_3) + \cos(b)(F_1 + F_4) \\ f_y = 0 \\ f_z = -\sin(a)(F_2 + F_3) - \sin(b)(F_1 + F_4) - (F_5 + F_6) \end{cases} \tag{4}$$

The joint force F_E in the earth coordinate system can be calculated by equation (5):

$$F_E = f_x \begin{bmatrix} \cos(\theta)\cos(\psi) \\ \cos(\theta)\sin(\psi) \\ -\sin(\theta) \end{bmatrix} + f_z \begin{bmatrix} \sin(\phi)\sin(\psi) + \cos(\phi)\sin(\theta)\cos(\psi) \\ -\sin(\phi)\cos(\psi) + \cos(\phi)\sin(\theta)\sin(\psi) \\ \cos(\phi)\cos(\theta) \end{bmatrix} + \begin{bmatrix} 0 \\ 0 \\ G \end{bmatrix} \tag{5}$$

The linear motion equation of the aircraft in the earth coordinate system can be determined from equation (6):

$$\begin{bmatrix} \ddot{x} \\ \ddot{y} \\ \ddot{z} \end{bmatrix} = \frac{f_x}{m} \begin{bmatrix} \cos(\theta)\cos(\psi) \\ \cos(\theta)\sin(\psi) \\ -\sin(\theta) \end{bmatrix} + \frac{f_z}{m} \begin{bmatrix} \sin(\phi)\sin(\psi) + \cos(\phi)\sin(\theta)\cos(\psi) \\ -\sin(\phi)\cos(\psi) + \cos(\phi)\sin(\theta)\sin(\psi) \\ \cos(\phi)\cos(\theta) \end{bmatrix} + \begin{bmatrix} 0 \\ 0 \\ g \end{bmatrix} \tag{6}$$

2.3. Angle kinematic equations

Under the effect of moment, the aircraft rotates around the centre of mass. At the hovering and take-off states, owing to the small mass and volume, moment of inertia of the rotor is very small, so the influence of the gyro effect can be ignored. When taking off, the aircraft is at a very low speed, so the air resistance proportional is also negligible. Therefore, only the torques generated by rolling, pitching and yawing are taken into account, which are represented by L, M, and N, respectively:

$$\begin{cases} L = \sin(a)(F_2 - F_3)r_1 + \sin(b)(F_1 - F_4)r_2 + (F_5 - F_6)R \\ M = (F_5 + F_6)l_1 - \left[\sin(a)(F_2 + F_3) + \sin(b)(F_1 + F_4)\right]l_2 \\ N = \cos(a)(F_2 - F_3)r_1 + \cos(b)(F_1 - F_4)r_2 \end{cases} \tag{7}$$

According to $\mathrm{M} = \mathrm{I}\dot{W}_B + W_B \times IW_B$:

$$\begin{cases} L = \dot{p}I_x + qr(I_z - I_y) - (\dot{r} + pq)I_{xz} \\ M = \dot{q}I_y + pr(I_x - I_z) + (p^2 - r^2)I_{xz} \\ N = \dot{r}I_z + pq(I_y - I_x) + (qr - \dot{p})I_{xz} \end{cases} \tag{8}$$

In the body coordinate system,I_x, I_y, I_z are moments of inertia in the direction of X, Y, and Z, and $I_{xz}$is the product of inertia of the axes x and z of the aircraft body. Because the mass of the aircraft is constant, each moment of inertia and inertial product are constant, so each coefficient in equation (5) can be replaced by C_1-C_9.

$$\begin{cases} \dot{p} = (c_1 r + c_2 p)q + c_3 L + c_4 N \\ \dot{q} = c_5 pr - c_6(p^2 - r^2) + c_7 M \\ \dot{r} = (c_8 p - c_2 r)q + c_4 L + c_9 N \end{cases} \tag{9}$$

3. Dynamic equation modeling

Based on equations (3), (6) and (9), the nonlinear dynamics model of the aircraft can be derived.

$$\begin{cases} \ddot{x} = \dfrac{f_x\cos(\theta)\cos(\psi) + f_z\left[\sin(\phi)\sin(\psi) + \cos(\phi)\sin(\theta)\cos(\psi)\right]}{m} \\ \ddot{y} = \dfrac{f_x\cos(\theta)\sin(\psi) + f_z\left[\cos(\phi)\sin(\theta)\sin(\psi) - \sin(\phi)\cos(\psi)\right]}{m} \\ \ddot{z} = \dfrac{-f_x\sin(\theta) + f_z\cos(\phi)\cos(\theta)}{m} + g \\ \dot{p} = (c_1 r + c_2 p)q + c_3 L + c_4 N \\ \dot{q} = c_5 pr - c_6(p^2 - r^2) + c_7 M \\ \dot{r} = (c_8 p - c_2 r)q + c_4 L + c_9 N \\ \dot{\phi} = p + \left(r\cos(\phi) + q\sin(\phi)\right)\tan(\theta) \\ \dot{\theta} = q\cos(\phi) - r\sin(\phi) \\ \dot{\psi} = \dfrac{1}{\cos(\theta)}\left(r\cos(\phi) + q\sin(\phi)\right) \end{cases} \tag{10}$$

Linearizing the nonlinear dynamics model of the aircraft in hovering state [5-6], the system can be defined as follows:

$$\begin{cases} \dot{X} = AX + Bu \\ Y = CX + Du \end{cases} \tag{11}$$

Where: X is a state variable, Y is the system output, u is the input vector, and the state space matrixes A, B, C, D are functions of time-varying parameters. X, Y, u are defined respectively as:$\mathrm{X} = \left[\dot{x}, \dot{y}, \dot{z}, \dot{\phi}, \dot{\theta}, \dot{\psi}, \phi, \theta, \psi\right]^T$,$\mathrm{Y} = [\phi, \theta, \psi]^T$,$\mathrm{u} = [u_1, u_2, u_3]^T$

$$\begin{cases} u_1 = \dfrac{c_3}{c_4}L + N \\ u_2 = M \\ u_3 = \dfrac{c_9}{c_4}N + L \end{cases} \tag{12}$$

Laplace transform is performed on equation (11):

$$G(\mathrm{s}) = C(sI - A)^{-1}B + D \tag{13}$$

Equilibrium computation shows that, in order to meet the requirements of vertical take-off and hovering and achieve a balance between force and moment during the vertical take-off to hovering phase, the aircraft needs to maintain an angle of 40°-60° with the ground. Afterwards, a set of trim points in the hovering state are obtained [7-8], and the pitch angle for the trim points is 60°.
After the linearization process, the transfer function can be developed.

$$G(\mathrm{s}) = \begin{bmatrix} \dfrac{c_4}{s^2} & 0 & \dfrac{433c_4}{250s^2} \\ 0 & \dfrac{c_7}{s^2} & 0 \\ 0 & 0 & \dfrac{2c_4}{s^2} \end{bmatrix} \tag{14}$$

According to $\mathrm{Y}(s) = G(s)u(s)$, the transfer function relationship between pitching moment and pitching angle can be expressed as:

$$\theta = \frac{c_7}{s^2}M = \frac{3.846}{s^2}M \tag{15}$$

4. Design of the PID control criterion

PID controllers have simple control structure and are easier to set in practical applications. Therefore, the PID controller is used to control the pitch angle. PID controller schematic diagram [9] is shown in Figure 3.

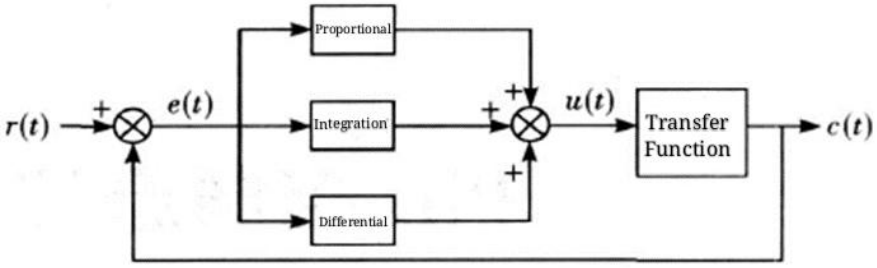

Figure 3. PID controller principle

Rise time, overshoot, settling time, and steady-state error are indicators to measure the performance of a control system. These four parameters reflect the system's responsiveness and stability, through which the performance of a system can be determined. With step response, the desirable performance specifications of the control system designed in this paper include the settling time which is less than 2 s, the overshoot which is less than 20%, and the rise time which is less than 1 s.

Based on the transfer function, the PID control strategy for pitch angle control is designed. The simulation with MATLAB/SIMULINK software verifies the correctness of the PID control strategy. Simulation block diagram is descripted in Figure 4. Parameter setting is crucial for PID control strategy. In this paper, the proportion degree method [10] is used to set the PID parameters. The parameters of the PID controller are $K_P = 1.5$, $K_I = 0.06$ and $K_D = 0.3$. In the actual simulation process, the parameters may be also adjusted by the root locus method and finally determined by the limit value range of the PID parameter in the outer-loop attitude control loop of flight control system. Simulation results are shown in Figure 5. Results indicate that the PID control strategy can basically meet the control requirements and achieve stable control of the pitch angle.

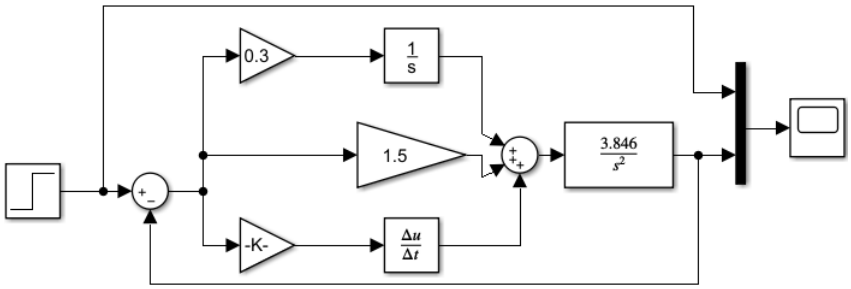

Figure 4. Pitch angle attitude simulation of the PID controller

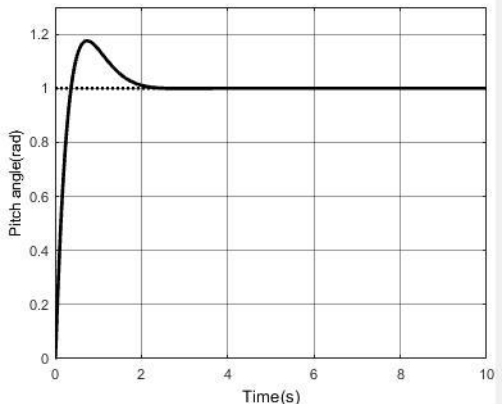

Figure 5. The pitch angle response curve under step input

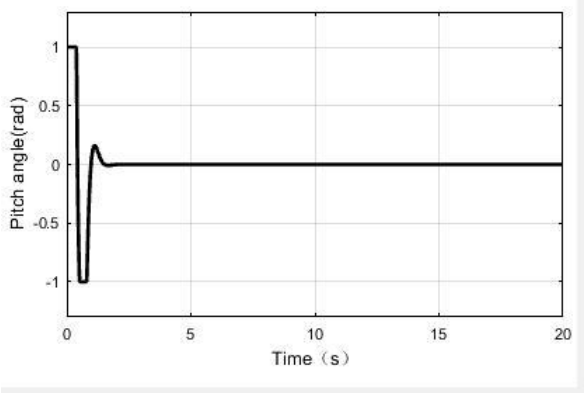

Figure 6. Changing curve of the pitch angle versus time

Finally, based on the Pixhawk flight controlling unit, the flight dynamics simulation model of the aircraft under the hovering state is constructed. The control amount of each channel for a set of trim and the PID parameters obtained by setting are input into the attitude angle control loop in the simulation model to obtain the simulation curve. As shown in Figure 6, with settling time less than 2 s, rise time less than 1 s and overshoot less than 20%, the simulation results reveal that the pitch attitude angle of the V/STOL aircraft under the hovering state is controllable and stable.

5. Conclusion

In this paper, the dynamics model built for the hovering and take-off phases of a new type of V/STOL UAV which is based on the principle of the increasing effect of deflection slip flow of the propeller aided by the forward vertical propeller is performed. Under the MATLAB/Simulink environment, the simulation model of PID controller is established and verify the control effect of PID controller. Results of the simulation suggest that this PID control system based on the vertical take-off and landing stage of the new V/STOL aircraft has good control effect and could achieve the stable control for pitch attitude.

References

[1] David L and Koldman 1981 *Introduction to V/STOL airplanes* (Iowa: Iowa State University Press)
[2] Herrero J L 2001 *Int. Society for Air Breathing Engines*
[3] Longyang Pan 2016 *Beijing Society of Theoretical and Applied Mechanics (Beijing)* vol 7 pp 60-61
[4] Kendoul F and Fantoni I and Lozano R 2005 *J. Helicopter Society Annual Forum* vol 61(1) pp 2-3
[5] WANG Qing and WANG Tong and HOU Delong 2014 *J. System Engineering and Electronic* vol 36(6) pp 1130-1136
[6] Wang Zhenchao and Peng Mingyan and Zhang Jinpeng and Yang Lingyu and Zhang Jing 2015 *J. AEO WEAPONY*. vol 1 pp 14-20
[7] ZHANG Zhi-Sheng and CHEN Huai-Min and WU Cheng-Fu and MA Song-Hui 2010 *J. Fire Control& Command Control.* vol 35(9) pp 93-97
[8] TANG Bin and HUANG Yi-Min 2007 *J. of Shenyang Institute of Aeronautical Engineering.* vol 24(1) pp 13-16
[9] Kendoul F and Fantoni I and Lozano R 2005 *Decision and Control, 2005 and 2005 European Control Conference* pp 8144-8149
[10] QIU Li and ZENG Gui and ZHU Xue and Sun Pei 2005 *J. Techniques of Automation and Application* vol 24(11) pp 28-31